Electrochemical tip-enhanced Raman spectroscopy imaging with 8 nm lateral resolution

Thomas Touzalin, Suzanne Joiret, Ivan T. Lucas, Emmanuel Maisonhaute

Electrochemical tip-enhanced Raman spectroscopy imaging with 8 nm lateral resolution

Thomas Touzalin, Suzanne Joiret, Ivan T. Lucas, Emmanuel Maisonhaute**

Sorbonne Université, CNRS, Laboratoire Interfaces et Systèmes Electrochimiques, LISE, F-75005, Paris, France.

AUTHOR INFORMATION

Corresponding Author

* E-mail: ivan.lucas@sorbonne-universite.fr

* E-mail: emmanuel.maisonhaute@sorbonne-universite.fr

Keywords : Tip Enhanced Raman Spectroscopy, Scanning Tunneling Microscopy, Nanospectroscopy, Electrochemistry, Plasmonics

Abstract

Herein, we report tip-enhanced Raman spectroscopy (TERS) hyperspectral imaging under electrochemical control of a non-Raman-resonant molecular compound. A new setup combining a Scanning Tunneling Microscope (STM) and an optical coupling with high signal excitation and collection efficiency enables fast chemical imaging of an opaque functionalized electrode surface upon polarization. Variations in the TERS signal intensity up to 1.8 were observed across the

surface, and correlated with topographic heterogeneities. These fluctuations, attributed to enhancement of the local electromagnetic field below the TERS tip, were used to estimate the lateral resolution of the produced hyperspectral image, which was found greater than 8 nm. This work represents an important step towards the use of electrochemical TERS imaging as a unique tool to unravel electrochemical processes at the nanoscale.

1. Introduction

Understanding the reactivity of complex electrode-electrolyte interfaces in an electrochemical environment at the nanometer scale is crucial to optimize the design of electrode materials with catalytic properties for instance. Various *in situ* approaches have already been proposed to scrutinize the properties of functional materials under their operating conditions. Scanning Tunneling Microscopy (STM) and Atomic Force Microscopy (AFM) have demonstrated spatial resolution down to the atomic scale and are commonly implemented in liquids and under electrochemical conditions.[1] Derived from these scanning probe methods, Scanning Electrochemical Microscopy (SECM) and associated techniques performed with nanoelectrodes allow to screen the local electrochemical reactivity of an interface.[2] *In situ* characterization of material at the nanoscale is also accessible with Liquid Cell Transmission Electron Microscopy (LCTEM). This approach, already successfully applied to various electrochemical systems[3-5], requires a fine control of the electron dose to minimize possible interference with the processes under study of the radiolytic species created by the high energy electron beam.[6] Super-resolved optical microscopy (ultimately providing 3D dynamic imaging) may also be used to track the behavior of individual electroactive nanoobjects at the vicinity of the electrode.[7-9] Nevertheless, none of these techniques enables chemical identification, which is crucial for elucidating local reactivity. This information may be retrieved through vibrational spectroscopies, and more specifically through Raman measurements that can be readily implemented in electrochemical conditions.[10] Whereas standard microRaman imaging is diffraction-limited and thus restricted to a lateral resolution of 200-300 nm using visible excitation, the nanometer scale characterization can be attained by resorting to Tip-Enhanced Raman Spectroscopy (TERS).[11-13] In TERS, a gold or silver STM or AFM tip apex is

illuminated to act as a local antenna that amplifies the local electromagnetic field, thus the spectroscopic response, while tracking the sample topography. TERS imaging, as near-field spectroscopy imaging provide a nanometric lateral resolution together with an excellent sensitivity. Single nanoobjects such as carbon nanotubes could be imaged in air,[14] while submolecular resolution was obtained in ultra-high vacuum at low temperature and with tailored tips to optimize the localized surface plasmon resonance.[15]

Implementation of TERS under electrochemical conditions has been already demonstrated but remains challenging. For top or side signal excitation/collection on opaque samples, the alteration of the optical path at the air/liquid interface is a major impediment.[16-18] For bottom illumination/collection on transparent samples, the minimization of the signal originating from the illuminated sample area (*i.e.* 1µm²) to extract only the signal at the TERS tip requires optimized sample/tip preparation and excitation/collection strategies.[19, 20] Different experimental configurations have allowed to investigate potential-dependent protonation states[16] or reorientation of molecules[21], to track electrochemical individual events at the tip-sample junction[20, 22], or to map surface redox potential distribution.[23] Back in 2016, we proposed the first set-up to implement TERS imaging in liquid and demonstrated hyperspectral imaging of a molecular assembly on a non-transparent substrate[24] in an organic solvent. Carbon nanotubes imaging in water (transparent sample) with a 30 nm resolution was also achieved by Kumar et al.[25] In 2017, we introduced the use of a water immersion objective with large numerical aperture for TERS measurements, to ease the laser focusing on the tip and to improve the TERS signal collection efficiency.[18, 26] We could thereby follow the electrochemical (EC) reduction of 4-nitrothiophenol self-assembled on a TERS active tapered electrode (EC-Tip-SERS), while Ren *et al.* improved the sensitivity of their EC-TERS

configuration in 2019.[27] Electrochemical TERS imaging has been very recently achieved in the AFM mode using a 3-electrode cell, a Raman-resonant molecular probe and a transparent sample,[23] yet EC-TERS imaging on non-transparent sample has not been demonstrated.

In this work, we describe a 4-electrode EC-setup adapted from our previous EC-Tip-SERS configuration to implement STM-TERS imaging on an opaque sample immersed in an electrolyte. To assess the imaging capabilities of this *in situ* setup, we selected a non-transparent substrate homogeneously covered with a non-electroactive molecular compound (non-Raman-resonant) and rely on the variations of the TERS intensity associated to changes in the tip-sample electromagnetic coupling across the scrutinized surface to determine the lateral resolution.

2. Results and discussion

The novel approach we propose is described in Figure 1 (additional details are provided in SI). A 40x water immersion objective (N.A. 0.8, working distance 3.3 mm) was immersed vertically in the EC-cell. In this setup designed for the analysis of non-transparent samples in liquid environments, no air-liquid interface distorts the optical path; the signal excitation and collection efficiency using this 40x water immersion objective was found to be higher than the one achievable in the air using a 100X long working distance objective[28] (N.A. 0.7, working distance 7 mm) on a silicon substrate (Figure S1a). A tip holder was designed so that the TERS-active STM tip could be brought at the focal point of the objective at an angle of 45° while being immersed in the liquid cell. While the TERS probe is maintained at a fixed position, the precise positioning of the laser at the tip apex through the objective and the sample displacements are insured by two independent piezo stages operating in the three directions XYZ. As mechanical couplings between the tip, the substrate and the objective are minimized in our set up, the optical

alignment is not compromised upon sample scanning and TERS mapping of a few µm² area is accessible.

An azobenzenethiol derivative **1** (cf. Figure 1b), often used as a reference system in TERS measurements [24, 29, 30], was self-assembled (SAM) on a gold-coated mica substrate. A greater TERS signal enhancement and higher imaging resolution [19, 31] of the SAM can be achieved at the gold tip/gold substrate junction, within this so-called gap-mode configuration. A 15 mm diameter O-ring was glued directly onto the substrate to be used as a small volume (ca. 1 mL) EC STM cell, filled with a 50 mM Na_2SO_4 solution. A ring-shaped gold counter-electrode and a silver pseudo-reference electrode were also added. The low-noise STM current amplifier was used to extract the current at the TERS active tip (*working electrode 1* kept at the virtual ground) while the substrate (*working electrode 2*), counter and reference electrodes were directly connected to a home-made bipotentiostat. Substrate and tip potentials can thus be adjusted versus the reference electrode, and be set independently, while controlling the STM bias voltage between both. The insulation of the tip and of the holder with varnish was optimized to decrease the leakage electrochemical current far below (less than 20 pA) the tunneling current setpoint used in STM imaging as feedback parameter for the control of the tip-sample distance (ca. 400 pA) [17]. Also, applied potential $E_{sample} = 0$ V and $E_{tip} = 0.2$ V *vs* Ag were selected to prevent gold electrooxidation and oxygen electroreduction while providing a 200 mV bias ($E_{tip} - E_{sample}$) sufficient to produce a net tunneling current flow.

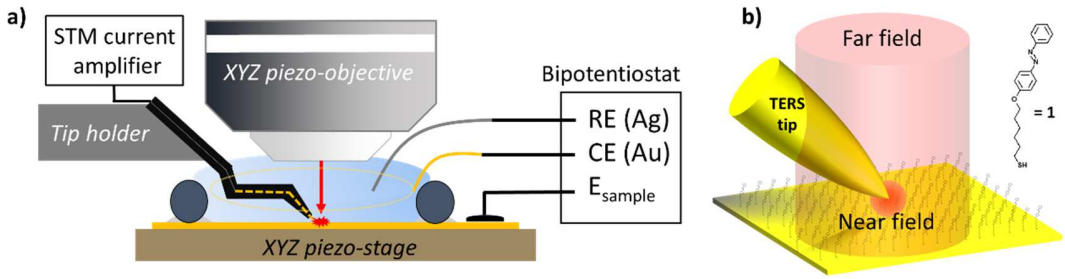

Figure 1. a) Electrochemical STM-TERS cell for top illumination and collection through a water immersion objective. A polarized TERS tip (*working electrode 1*: potential E_{tip} *vs* Ag), partially insulated, is brought to contact to the conductive sample (*working electrode 2*: potential E_{sample} *vs* Ag) at a 45° angle. A gold ring and a silver wire are used as counter and pseudo-reference electrodes respectively. **b)** Depiction of the SAM (azobenzenethiol derivative **1**) functionalized gold surface and of the signal enhancement at tip-sample junction (near-field optical coupling).

Despite the long lever arm formed by the bended STM probe and the presence of the immersion objective, high quality STM imaging could be recorded in the electrolyte under potential control as depicted in Figure 2a. STM images exhibits sharp edges between adjacent gold terraces created upon flame annealing and also characteristic gold vacancy islands ("pits" with depth of one or several gold atoms ~ 0.3 - 0.9 nm and diameter of *ca.* 5 nm), created by the gold surface reconstruction due to formation of thiolate-gold complexes upon sulfur species adsorption (Figure 2b).[32, 33] Another STM image recorded over a larger area is provided in Figure S2. These results comparable to those obtained in the air on similar samples evidence that this new holder and tip design do not alter the mechanical stability of the STM/Raman coupled system in liquid, prerequisite to any EC STM-TERS imaging with high lateral and vertical resolution.

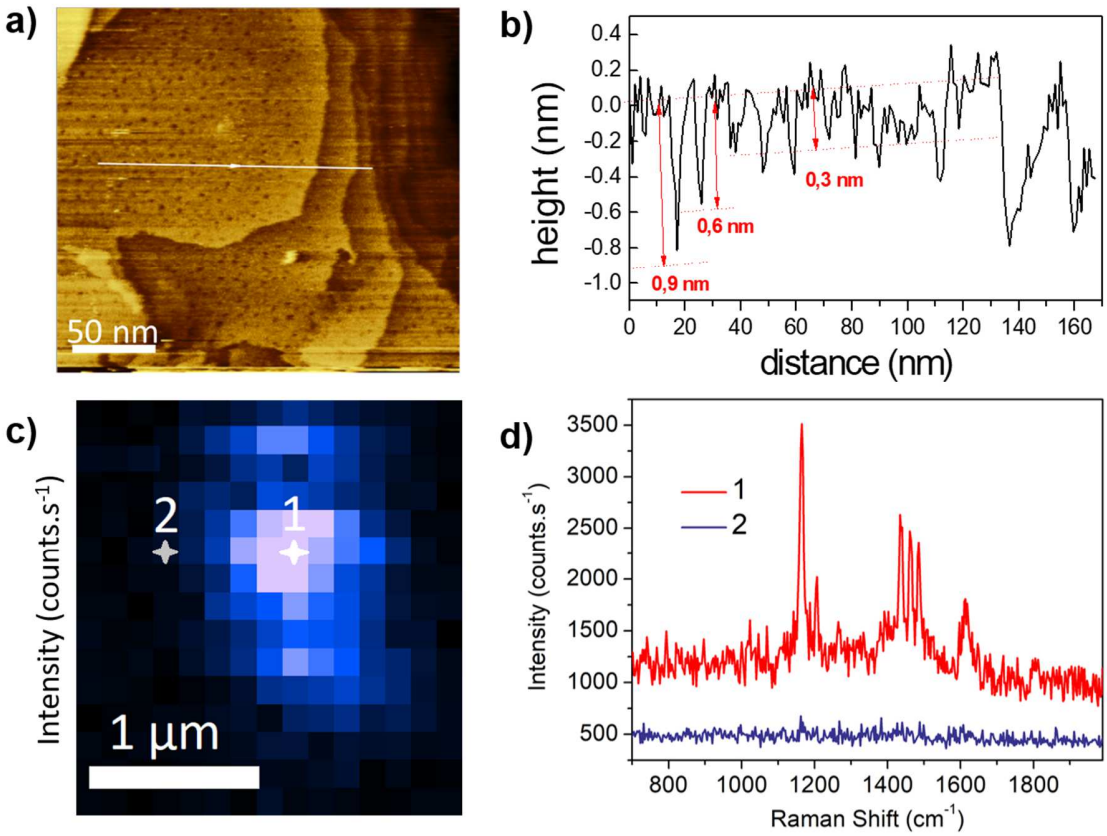

Figure 2. Independent evaluation of EC-STM stability and EC-TERS efficiency - **a)** EC STM imaging (200x200 nm²) of a gold electrode functionalized with the azobenzenethiol derivative **1** in a 50 mM Na_2SO_4 solution (E_{sample} = 0 V vs Ag, bias = 200 mV, i_{tunnel} = 400 pA); **b)** height profile along the white line on 2a); **c)** 2.4×2.4 µm² XY objective map highlighting the localized hot spot at the apex of the TERS tip in liquid (intensity of the 1143 cm^{-1} band); **d)** near-field (1: red, at the apex of the tip) and far-field (2: blue, 1 µm away from the apex of the tip). Laser power: 130 µW, acquisition time: 500 ms.

The optical image presented in Figure S3 shows that a precise focusing of the laser on the tip apex can be realized through the immersion objective attached to a XYZ piezo stage. Scanning of the laser in XY, XZ, YZ planes (objective maps) allows identification of the "hotspot" at the

tip apex in close vicinity with the substrate, *i.e.* the position associated to the highest TERS signal enhancement. The XY objective map presented in Figure 2c, which depicts the intensity of the 1143cm^{-1} Raman band of **1** (see Fig. 2d), shows that the largest Raman intensity originates from a limited region of about 1µm around the tip apex. As seen on Figure 2d, strong intensity Raman signatures of **1** can be extracted through 3.3 mm of electrolyte at short acquisition time (0.5 s) and minimal laser power (130 µW) when the tip is in contact with the sample (near-field spectrum). Additional contribution of the surrounding electrolyte (the symmetric stretching mode of SO_4^{2-}) can also be detected in some cases as shown in Figure S4 recorded with a different TERS tip. In this case the far-field spectrum is recorded by increasing the tip-sample distance to 100 nm so that the laser can be still focused on the sample but the near-field coupling of the tip is lost[34] and thus the signature of **1** disappears This confirms that the enhancement process inherent to the presence of the tip in the close vicinity of the sample no longer takes place.

Fast hyperspectral EC-TERS imaging was then achieved across a 365×120 nm² area of the SAM functionalized gold substrate. While Raman signatures of **1** were observed all over the scrutinized area, some signal intensity variation were however detected. The TERS map obtained by integration of the peak at 1143 cm^{-1} and the STM map shown on Figure 3a and b reveals a stripe of strong Raman intensity along the edge of a substrate topographic line (gold step between two adjacent terraces). This correlation between topographic and vibrational information is highlighted in Figure 3c in the line profile extracted from the STM and the TERS intensity maps along the line (area of the 1143 cm^{-1} band: A_{1143}). Raman bands with intensity *ca.* 1.8 fold higher than on the terrace region were observed at the edge of the gold step on a distance corresponding to two pixels (2×7.3 nm), the overall transition occurring within 30 nm. This additional enhancement, clearly visible in individual raw data spectra collected across the line in

Figures 3a and 3b, is not associated to any shift in energy of the Raman bands, neither to a variation of the relative intensity of the different bands nor to an increase of full width at half maximum (see Figure 3d). The same conclusions were reached after further analysis consisting in fitting the peaks by Lorentzian functions[35] and then dividing the peak intensity by the background one as suggested by Ren et al (see SI for a complete analysis).[36]

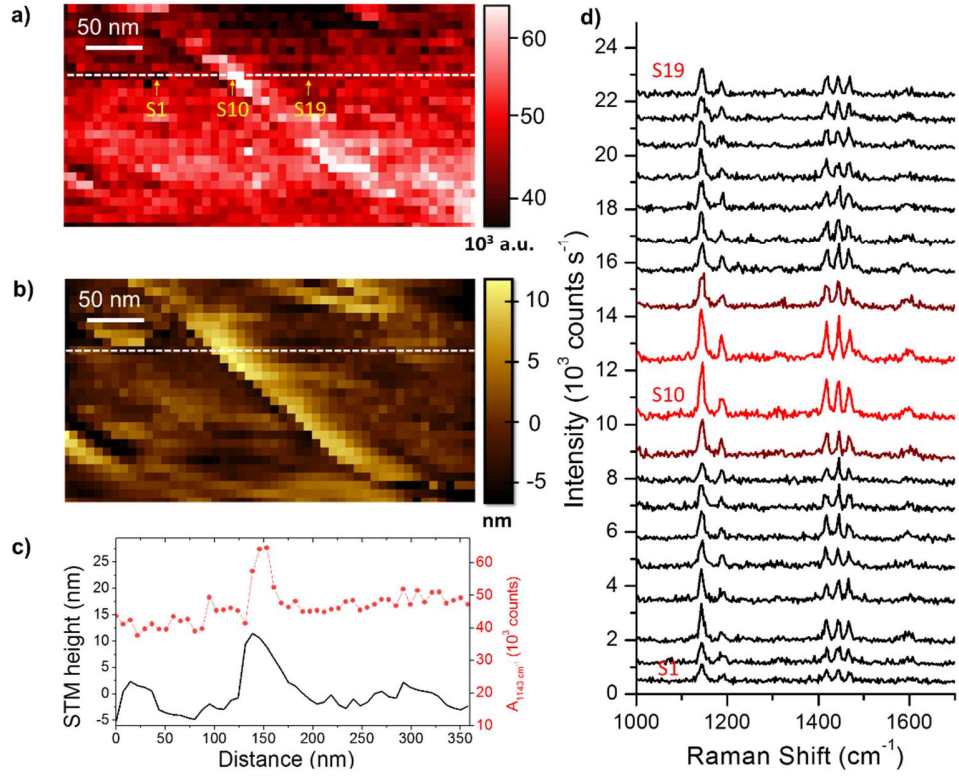

Figure 3. 365x120 nm² EC STM-TERS imaging of a gold surface functionalized with **1** in 50 mM Na_2SO_4. **a)** EC TERS map of the 1143 cm^{-1} mode (area); **b)** EC STM map recorded during TERS imaging; **c)** EC TERS (red) and STM (grey) profiles along the line on 3a) and b); **d)** EC TER spectra at positions indicated on 3b) (1: yellow, 2: red). E_{sample}: 0 V *vs* Ag, bias voltage: 200 mV, i_{tunnel}: 400 pA, laser power: 130 µW, integration time: 500 ms/px. Spectra are offset for clarity.

Such fluctuations of the TERS signal intensity at gold steps have been already reported in the air and are explained by the additional enhancement of the local electric field due to the change in optical coupling between the tip and the sample at the step edges.[37-39] Any additional involvement of a change in molecule orientation or packing at the edge is difficult to ascertain since the spectra still result from contributions over a pixel area of 7.3×7.3 nm^2, thus including molecules not at the edge. Since pronounced intensity changes are appreciable over one pixel distance, our results suggest that the lateral resolution of our TERS setup is greater than 8 nm. As similar effects can be expected on any nanosize features of complex surfaces, *e.g.* onto electrocatalytic surfaces, fluctuations in TERS intensity upon polarization should be considered carefully in the future, especially during *operando* measurements, to distinguish between local variation in the scatterer density (inhomogeneous molecular coverage, desorption upon polarization), of their orientation and of their composition (molecular transformation), and between local alteration of the electric field at geometrical singularity below the tip, possibly combined with interdependent potential effects *i.e.* reorganization of the double layer, specific adsorption, modification of local electron density. It may also be of prime importance to understand the impact on the TERS signatures of the explored electrochemical potential and possibly of "hot electrons" produced at the tip-sample junction which may induce unexpected chemical reactions.

3. Conclusions

We introduced in this work a coupled electrochemical STM-TERS system which allows imaging of an electrochemical interface under potential control with a lateral resolution of 8 nm. The proposed set-up provides robust EC-STM imaging as demonstrated onto a functionalized gold surface. Through the use of a water immersion objective and the development of a

dedicated EC-STM cell, high excitation and collection efficiency of the TERS signal is achieved, enabling fast hyperspectral TERS imaging of non-Raman-resonant molecular compounds in liquid and upon polarization. Local variations of the TERS signal intensity were observed across the sample surface and interpreted as modulation of the local electromagnetic field on nanosize features at the TERS tip-substrate junction. We expect to reach imaging resolution and sensitivity close to those reached in the air in the near future. These results pave the road for composition imaging of complex interfaces at the nanoscale and for TERS analysis of potential-driven reactions occurring for instance in battery materials or at electrocatalytic sites. Further experiments need to be carried out to investigate the influence of electrochemical conditions on TERS mechanism, *i.e.* on the modulation of plasmonic properties of the tip and sample under polarization in an electrolyte medium.

ASSOCIATED CONTENT

Supporting Information. Details of tip, surface and cell preparation, reference measurements onto a silicon wafer, additional STM image, optical image of the TERS tip in STM contact with the substrate, hot spot identification with a different tip, further analysis of the hyperspectral TERS image (PDF).

The following files are available free of charge.

AUTHOR INFORMATION

* E-mail: ivan.lucas@sorbonne-universite.fr

* E-mail: emmanuel.maisonhaute@sorbonne-universite.fr

ORCID

Emmanuel Maisonhaute: 0000-0001-6337-7436

Ivan T. Lucas: 0000-0001-8930-0437

Notes

The authors declare no competing financial interests.

ACKNOWLEDGMENTS

This work was funded by Sorbonne Université, CNRS, the FP7-People program (CIC - ID: 618643) of the European Union, the Labex "MiChem" (ANR-11-IDEX-0004-02), the Region Ile de France through the framework DIM Nano-K, and the French National Research Agency (project ANR- 17-CE07-0012-01).

REFERENCES

[1] C.J. Chen, Introduction to Scanning Tunneling Microscopy: Second Edition, Oxford University Press, Oxford, 2007.
[2] M.A. O'Connell, A.J. Wain, Mapping electroactivity at individual catalytic nanostructures using high-resolution scanning electrochemical–scanning ion conductance microcopy, Anal. Chem., 86 (2014) 12100-12107.
[3] M.J. Williamson, R.M. Tromp, P.M. Vereecken, R. Hull, F.M. Ross, Dynamic microscopy of nanoscale cluster growth at the solid−liquid interface, Nat. Mater., 2 (2003) 532-536.
[4] F.M. Ross, Opportunities and challenges in liquid cell electron microscopy, Science, 350 (2015) aaa9886.
[5] P. Abellan, B.L. Mehdi, L.R. Parent, M. Gu, C. Park, W. Xu, Y.H. Zhang, I. Arslan, J.G. Zhang, C.M. Wang, J.E. Evans, N.D. Browning, Probing the degradation mechanisms in electrolyte solutions for Li-ion batteries by in situ transmission electron microscopy, Nano Lett., 14 (2014) 1293-1299.

[6] E. Sutter, K. Jungjohann, S. Bliznakov, A. Courty, E. Maisonhaute, S. Tenney, P. Sutter, In situ liquid-cell electron microscopy of silver-palladium galvanic replacement reactions on silver nanoparticles, Nat. Commun., 5 (2014) 4946.
[7] V. Brasiliense, P. Berto, C. Combellas, G. Tessier, F. Kanoufi, Electrochemistry of single nanodomains revealed by 3D holographic microscopy, Accounts Chem. Res., 49 (2016) 2049-2057.
[8] A.N. Patel, A. Martinez-Marrades, V. Brasiliense, D. Koshelev, M. Besbes, R. Kuszelewicz, C. Combellas, G. Tessier, F. Kanoufi, Deciphering the elementary steps of transport-reaction processes at individual Ag nanoparticles by 3D super localization microscopy, Nano Lett., 15 (2015) 6454-6463.
[9] V. Brasiliense, P. Berto, P. Aubertin, E. Maisonhaute, C. Combellas, G. Tessier, A. Courty, F. Kanoufi, Light driven design of dynamical thermosensitive plasmonic superstructures: A bottom-up approach using silver supercrystals, ACS Nano, 12 (2018) 10833-10842.
[10] X. Wang, M.C. Bernard, C. Deslouis, S. Joiret, P. Rousseau, Kinetic reactions in thin polyaniline films revisited through Raman-impedance dynamic coupling, Electrochim. Acta, 56 (2011) 3485-3493.
[11] R.M. Stockle, Y.D. Suh, V. Deckert, R. Zenobi, Nanoscale chemical analysis by tip-enhanced Raman spectroscopy, Chem. Phys. Lett., 318 (2000) 131-136.
[12] T. Schmid, L. Opilik, C. Blum, R. Zenobi, Nanoscale chemical imaging using tip-enhanced Raman spectroscopy: A critical review, Angew. Chem.-Int. Edit., 52 (2013) 5940-5954.
[13] X. Wang, S.C. Huang, T.X. Huang, H.S. Su, J.H. Zhong, Z.C. Zeng, M.H. Li, B. Ren, Tip-enhanced Raman spectroscopy for surfaces and interfaces, Chem. Soc. Rev., 46 (2017) 4020-4041.
[14] C. Chen, N. Hayazawa, S. Kawata, A 1.7 nm resolution chemical analysis of carbon nanotubes by tip-enhanced Raman imaging in the ambient, Nat. Commun., 5 (2014) 3312.
[15] R. Zhang, Y. Zhang, Z.C. Dong, S. Jiang, C. Zhang, L.G. Chen, L. Zhang, Y. Liao, J. Aizpurua, Y. Luo, J.L. Yang, J.G. Hou, Chemical mapping of a single molecule by plasmon-enhanced Raman scattering, Nature, 498 (2013) 82-86.
[16] Z.-C. Zeng, S.-C. Huang, D.-Y. Wu, L.-Y. Meng, M.-H. Li, T.-X. Huang, J.-H. Zhong, X. Wang, Z.-L. Yang, B. Ren, Electrochemical tip-enhanced Raman spectroscopy, J. Am. Chem. Soc., 137 (2015) 11928-11931.
[17] N. Martín Sabanés, L.M.A. Driessen, K.F. Domke, Versatile side-illumination geometry for tip-enhanced Raman spectroscopy at solid/liquid interfaces, Anal. Chem., 88 (2016) 7108-7114.
[18] T. Touzalin, S. Joiret, E. Maisonhaute, I.T. Lucas, Capturing electrochemical transformations by tip-enhanced Raman spectroscopy, Curr. Opin. Electrochem., 6 (2017) 46-52.
[19] N. Kazemi-Zanjani, S. Vedraine, F. Lagugné-Labarthet, Localized enhancement of electric field in tip-enhanced Raman spectroscopy using radially and linearly polarized light, Opt. Express, 21 (2013) 25271-25276.
[20] D. Kurouski, M. Mattei, R.P. Van Duyne, Probing redox reactions at the nanoscale with electrochemical tip-enhanced Raman spectroscopy, Nano Lett., 15 (2015) 7956-7962.
[21] N.M. Sabanes, T. Ohto, D. Andrienko, Y. Nagata, K.F. Domke, Electrochemical TERS elucidates potential-induced molecular reorientation of adenine/Au(111), Angew. Chem.-Int. Edit., 56 (2017) 9796-9801.
[22] M. Mattei, G. Kang, G. Goubert, D.V. Chulha, G.C. Schatz, L. Jensen, R.P. Van Duyne, Tip-enhanced Raman voltammetry: Coverage dependence and quantitative modeling, Nano Lett., 17 (2017) 590-596.

[23] G. Kang, M. Yang, M.S. Mattei, G.C. Schatz, R.P. Van Duyne, In situ nanoscale redox mapping using tip-enhanced Raman spectroscopy, Nano Lett., 19 (2019) 2106-2113.
[24] T. Touzalin, A.L. Dauphin, S. Joiret, I.T. Lucas, E. Maisonhaute, Tip enhanced Raman spectroscopy imaging of opaque samples in organic liquid, Phys. Chem. Chem. Phys., 18 (2016) 15510-15513.
[25] N. Kumar, W. Su, M. Veselý, B.M. Weckhuysen, A.J. Pollard, A.J. Wain, Nanoscale chemical imaging of solid–liquid interfaces using tip-enhanced Raman spectroscopy, Nanoscale, 10 (2018) 1815-1824.
[26] T. Touzalin, S. Joiret, E. Maisonhaute, I.T. Lucas, Complex electron transfer pathway at a microelectrode captured by in situ nanospectroscopy, Anal. Chem., 89 (2017) 8974-8980.
[27] Z.-C. Zeng, S. Hu, S.-C. Huang, Y.-J. Zhang, W.-X. Zhao, J.-F. Li, C. Jiang, B. Ren, Novel electrochemical Raman spectroscopy enabled by water immersion objective, Analytical Chemistry, 88 (2016) 9381-9385.
[28] Z.-C. Zeng, S. Hu, S.-C. Huang, Y.-J. Zhang, W.-X. Zhao, J.-F. Li, C. Jiang, B. Ren, Novel electrochemical Raman spectroscopy enabled by water immersion objective, Anal. Chem., 88 (2016) 9381-9385.
[29] H.K. Wickramasinghe, M. Chaigneau, R. Yasukuni, G. Picardi, R. Ossikovski, Billion-fold increase in tip-enhanced Raman signal, ACS Nano, 8 (2014) 3421-3426.
[30] C. Toccafondi, G. Picardi, R. Ossikovski, Molecular bending at the nanoscale evidenced by tip-enhanced Raman spectroscopy in tunneling mode on thiol self-assembled monolayers, J. Phys. Chem. C, 120 (2016) 18209-18219.
[31] S.F. Becker, M. Esmann, K. Yoo, P. Gross, R. Vogelgesang, N. Park, C. Lienau, Gap-plasmon-enhanced nanofocusing near-field microscopy, ACS Photonics, 3 (2016) 223-232.
[32] C. Vericat, M.E. Vela, G. Benitez, P. Carro, R.C. Salvarezza, Self-assembled monolayers of thiols and dithiols on gold: new challenges for a well-known system, Chem. Soc. Rev., 39 (2010) 1805-1834.
[33] E. Pensa, C. Vericat, D. Grumelli, R.C. Salvarezza, S.H. Park, G.S. Longo, I. Szleifer, L.P. Méndez De Leo, New insights into the electrochemical desorption of alkanethiol SAMs on gold, Phys. Chem. Chem. Phys., 14 (2012) 12355-12367.
[34] G. Picardi, M. Chaigneau, R. Ossikovski, C. Licitra, G. Delapierre, Tip enhanced Raman spectroscopy on azobenzene thiol self-assembled monolayers on Au(111), J. Raman Spectrosc., 40 (2009) 1407-1412.
[35] B. Pettinger, K.F. Domke, D. Zhang, G. Picardi, R. Schuster, Tip-enhanced Raman scattering: Influence of the tip-surface geometry on optical resonance and enhancement, Surf. Sci., 603 (2009) 1335-1341.
[36] K.Q. Lin, J. Yi, J.H. Zhong, S. Hu, B.J. Liu, J.Y. Liu, C. Zong, Z.C. Lei, X. Wang, J. Aizpurua, R. Esteban, B. Ren, Plasmonic photoluminescence for recovering native chemical information from surface-enhanced Raman scattering, Nat. Commun., 8 (2017) 9.
[37] A. Merlen, J. Plathier, A. Ruediger, A near field optical image of a gold surface: a luminescence study, Phys. Chem. Chem. Phys., 17 (2015) 21176-21181.
[38] A. Bhattarai, A.G. Joly, W.P. Hess, P.Z. El-Khoury, Visualizing electric fields at Au(111) step edges via tip-enhanced Raman scattering, Nano Lett., 17 (2017) 7131-7137.
[39] W.H. Zhang, X.D. Cui, B.S. Yeo, T. Schmid, C. Hafner, R. Zenobi, Nanoscale roughness on metal surfaces can increase tip-enhanced Raman scattering by an order of magnitude, Nano Lett., 7 (2007) 1401-1405.

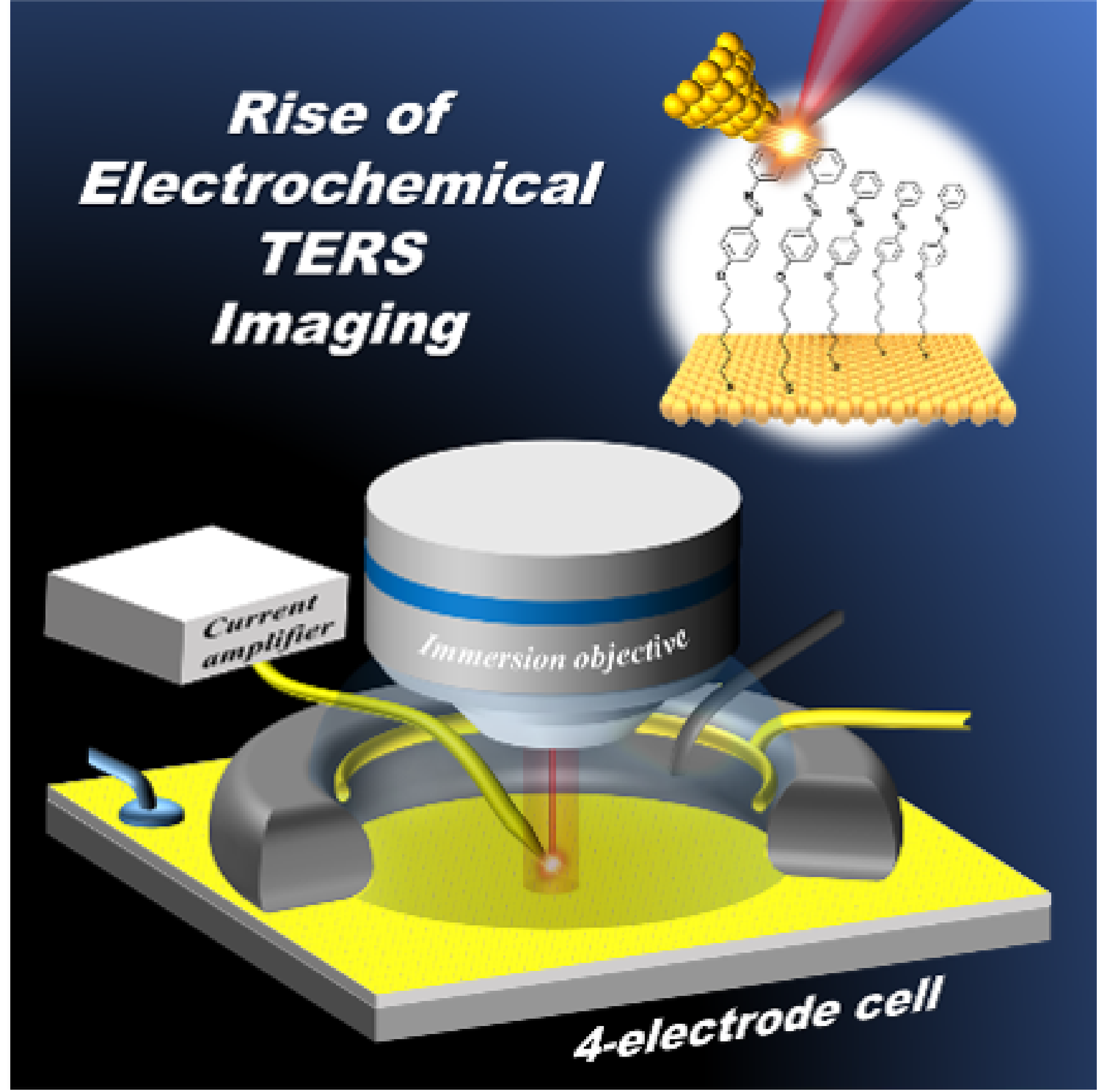
Rise of
Electrochemical
TERS
Imaging
Current amplifier
Immersion objective
4-electrode cell